Egyptian Journal of Chemistry

http://ejchem.journals.ekb.eg/

Antimicrobial Activity of Polymeric Surfactants Blending With Zinc Oxide Nanoparticles Derived From Electric Arc Furnace Dust

Ahmed I. Adawy,[1*] Ramadan M. Soliman,[2] Abdelghaffar S. Dhmees,[3] and Zizi I. Abdeen[4]

[1] Petrochemical Department, [2] Process Development Department, [3] Analysis & Evaluation Department, [4]Polymers Laboratory, Petrochemical Department, Egyptian Petroleum Research Institute (EPRI), Nasr City, Cairo,11727, Egypt.

Abstract

The biological activities of poly (ethylene glycols) (PEG) that esterified with lauric acid or myristic acid were enhanced by mixing with zinc oxide nanoparticles (ZnO-NPs) derived as of hazardous trash "Electric Arc Furnace Dust (EAFD)" which formed through steel fabrication using sodium hydroxide (NaOH). A diverse temperature was applied to characterize and examine the prepared polymeric surfactants those possess characteristics of surfactant and polymer together. The surface properties were measured and worked out. The hydrodynamic particle diameter normally maximized as the surfactant carbon numbers increased and at blending with ZnO-NPs as exhibited in the dynamic light scattering (DLS) statistics due to aggregation of molecules. The antimicrobial action against different microorganisms of all such designed structures was assessed and assigned. The results plain that, all such engineered nonionic polymeric surfactants possess good surface criteria and biological activity and blending them with ZnO-NPs to obtain polymeric surfactant nanocomposites for enhancing their biological activity against Gram-positive bacteria (*Bacillus subtilis* and *Staph*. *aureus*), Gram-negative bacteria (*P. aeruginosa* and *E. coli*), yeast (*Candida albicans*) and microalga (*Chlorella Vulgaris*).

Keywords: Zinc oxide nanoparticles; Esterification; Biological Activities; Surface properties; Polymeric surfactants; Nanocomposites

1. Introduction

Surfactants are distinguished by having exclusive chemical structure, that causes them extremely significant in a variety of sectors, both industrial and scientific, and they have stimulated the interest of researchers. The surfactant is an organic molecule that consists of two distinct polarities linked with each other; one portion is greatly polar and is known as the hydrophilic head, whereas the other is recognized for its strong hydrophobicity and is known as the hydrophobic tail[1, 2]. Surfactants are distinguished by their capacity to decrease surface tension between two distinct phases, one of which is liquid.

Surfactants have a distinctive structure that allows them to aggregate in micelles and/or adsorb at system interfaces for system stability, giving them an essential position in a wide range of vital applications like generating microemulsions., detergent, pharma-ceutical applications, emulsion polymerization, corrosion inhibitors, nanotechnology, drug delivery, emulsifier, enhancing oil recovery & biocide[3, 4].

Nonionic surfactants are thought to be one of the greatest environmentally friendly between the other forms of surface active agents[5]. Charged surfactants comprising cationic, anionic, zwitterionic and amphoteric possess risky environmental effect[6]. Surfactants, in specifically, could be employed as antimicrobial operators owing to their molecular structure and ability to engage with biological films[7]. Surfactant functions have expanded over the years to the sector of nanotechnology, wherever they are employed as potent agents for the production and customization of nanoparticles (NPs)[8]. The nanoparticles and surfactants combining together at the interfaces that generate a significant area of study particularly in the technology of enhancement the constancy of foams and emulsions[9]. The combination of nanoparticles

_____

_____

and surfactants would have a combined impact on biological networks as well as the environment.

The most important obstacle for using dry solid nanoparticles in different applications is its dispersion in liquid media. Nanofluids are colloidal suspensions of nanoparticles in stabilizing matrices that have gained popularity due to their numerous applications in many sectors[10]. Many researches are being conducted on the creation of dispersed metal oxides in various stabilizing media for the stability of nanoparticles on the one hand, and integrating the chemical and physical characteristics of their constituent materials on the other[11]. Similarly, hybrid materials composed of one or more nanoparticles dispersed in a base fluid offer numerous benefits over un-dispersed nanoparticles due to their synergistic impact. Polymers are an attractive substitute for the stability of metal oxide nanoparticles. Nanomaterials are able to be dispersed in a polymer matrix or chemically linked to it to produce a metal complex. Surfactants are also employed to stabilize nanoparticles since they may reduce the surface tension of fluids that maximize the immersion of the nanoparticles. Many literatures have been conducted on the function of surfactants in the stability of nanoparticles, with the benefit of avoiding rapid sedimentation[12,13].

The antimicrobial effectiveness of ZnO-NPs has currently been received a lot of attention[14]. Zinc is an essential nonferrous metal that is used in a variety of functions like batteries, solder, dielectric materials, and piezoelectric materials. Valorization of waste materials and industrial by-product such as, black liquor, iron/ steel making slag and dust to value-add chemicals[15] adsorbents[16], nanomaterials[17] catalysts[18] and anticorrosion[19] became a new trend due to the economics of biological and chemical processes. Electric arc furnace dust (EAFD) one of the most produced waste in steel industries. Where each one ton of steel produced about 20 kg of EAFD[17] EAFD composed mainly from Fe_2O_3, ZnO and $ZnFe_2O_4$ oxides.

In our work, nanostructure of non-ionic polymeric surfactants were designed through esterified of poly (ethylene glycol) (PEG) and lauric acid or myristic acid and their biological activities were improved through blending them with ZnO-NPs. Also, the aim of this present work is to recover zinc from spent electric arc furnace dust by means of sodium hydroxide alkali leaching and synthesis of ZnO-NPs. These nanostructure compounds were characterized by investigating their surface activities and structures. As well, the length of the field of hindrance technique in opposition to diverse microbes is used to evaluate and determine their biological activity.

2. Experimental Technique:

2.1. Materials:

The materials utilized right now had uncontaminated degree from Aldrich and utilized without extra filtration. The solvents utilized were of unpolluted class. Electric Arc Furnace Dust was purchased from El-EZZ company for Steel industries (El-Ain El-Sokhna, Suez). XRF analysis shows the mainly composition as follow (64.6% Fe_2O_3, 18.1% ZnO, 10.5% CaO, 5.7% SiO_2, 1.1% traces).

2.2. Designing of Nonionic surfactants [20]:

Polyethylene glycol 0.1 mole, Mw =600 was esterified by equimloar of saturated fatty acids (lauric acid and myristic acid) in xylene (150 mL) like a solvent. A 0.01% p‑toluene sulphonic acid joined in the reaction blend like a catalyst. The reaction progressed under warming state (140 ºC) awaiting the azeotropic quantity of water (0.1 mol, 1.8 mL collected. After that the solvent was withdrawn utilizing vacuum rotary evaporator. The catalyst was collected from the blend utilizing petroleum ether. Later consequent filtration was finished through methods of vacuum distillation to evacuate the remainder and lasting substances. The prepared esters were labeled as (Ia) and (IIa), for laurate and myristate in that order, Scheme (1).
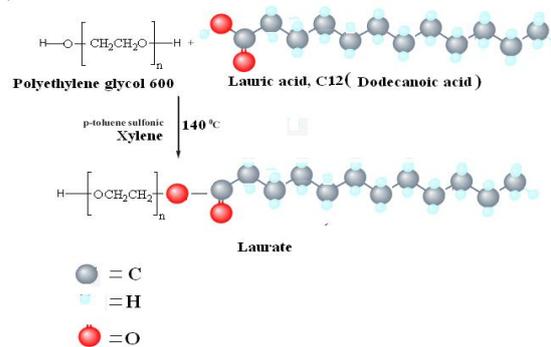
Scheme (1).

2.3. Zinc Oxide extraction from EAFD:

Zn was extracted from EAF dust sample by two integrated steps: EAF dust fusion with solid NaOH and then leaching, according to Youcai process [21] with some modification. Firstly, Fusion of EAF dust was done at 400°C for 1 h using a mass fraction of dust/NaOH (1:1). Then, a 5 mol L-1 NaOH solution was used to leach Zn from fused EAF dust. The leaching process takes 5h with stirring and reflux at 100ºC. Where the ZnO with alkali leaching convert to $Na_2Zn(OH)_4$ solution. According to Mehmet [22] the precipitation of Zn from the dissolved form was achieved with 5 M HCl (hydrochloric acid) solution under vigorous stirring at 60ºC at pH12.5 as shows in the equation:

_____

_____

$Zn(OH)_4^{2-} + 2HCl \rightarrow Zn(OH)_2 + 2Cl^- + 2H_2O$

The obtained $Zn(OH)_2$ was cleaned a lot by distilled water and ethanol before drying in 100°C overnight.

2.4. Synthesis of zinc oxide nanoparticle:

3 g of the extracted Zinc Oxide derived from EAFD was dissolved in 90 mL nitric acid 1 M at 100°C for form zinc nitrates $Zn(NO_3)_2$ before adding 10 mL of Ethylene glycol. The mixture was stirred for 30 minute. Then, 0.1 g of over the mixture polyvinyl alcohol PVA was added to prevent nanoparticles agglomeration. Then a solution of NaOH 1 mol L-1 in ethylene glycol inserted dropwise inside a previous prepared solution ($Zn(NO_3)_2$, EG and PVA) till pH 10 to full synthesis of zinc hydroxide $Zn(OH)_2$. After that, the colloidal solution warmed during reflux at 120 °C for 3 h. The obtained zinc oxide nanoparticles ZnO-NPs was centrifuged for 15 min at 6,000 rpm then cleaned several times by ethyl alcohol. The hard substance was calcined at 500°C for 4h for further characterization. However, the following equations summarized the overall chemical reaction for ZnO nanoparticles preparation by using NaOH:

$$Zn(NO_3)_{2(s)} + 2NaOH_{(s)} \longrightarrow Zn(OH)_{2(s)} + NaNO_{3(L)}$$

Zinc	Sodium	Zinc	Sodium
Nitrate	Hydroxide	Hydroxide	Nitrate

$$Zn(OH)_{2(s)} \xrightarrow{\Delta} ZnO_{(s)} + H_2O_{(L)}$$

Zinc	Zinc	
Hydroxide	Oxide	Step 2
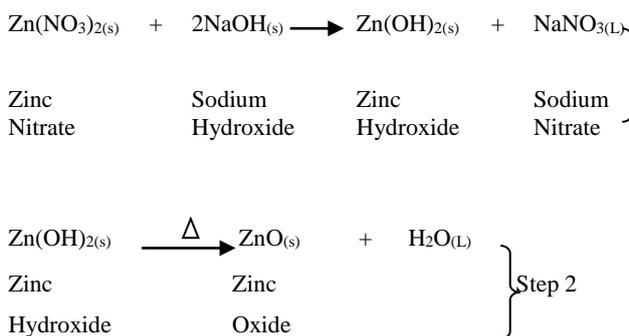
### 2.5. Preparation of the nanocomposite of non-ionic polymeric surfactants with ZnO nanoparticles:

The emulsion of nanoparticles (20 mL) merged with 5 mL saturated solution of designed nonionic surfactants (Ia, IIa) (0.01 mol) in distilled water. The mix was kept blending for 24 h until the color changes to shape surfactant nanostructures which marked as Ib and IIb [20, 23].

2.6. Structural verification of the synthesized surfactants:

The chemical structure of the designed nonionic surfactants was characterized through: FTIR spectra were developed utilizing ATI Mattsonm Infinity series™, Bench top 961 drove by Win First™ V2.01 software. (Egyptian Petroleum Research Institute).

Also, the crystal structure of the designed materials was verified utilizing X-ray diffraction (XRD) using ANalytical XPERT PRO MPD, Netherland. The angle range (2θ = 4-80°) scanned using a nickel-filtered Cu Kα radiation source with wave length of 0.154 nm). Energy dispersive x-ray spectroscopic (EDX) technique is used to detect the components of the NPs ZnO with an EDX detector (Oxford LINKISIS 300) outfitted on Environmental scanning electron microscope (ESEM, Philips type model XL30).

The Brunauer-Emmett-Teller (BET) surface area and Average pore diameter was estimated with N2 adsorption-desorption isotherms that were achieved with Quantachrome Nova 3200 instrument (USA).

Dynamic light scattering (DLS) compute the hydrodynamic diameter and zeta potential of the similar solution that utilized in EDX. It was characterized by dynamic light scattering (DLS) utilizing a Malvern Zetasizer Nano (Malvern Instruments Ltd., Worcestershire, UK). Every DLS estimation was operated in triplicate utilizing computerized, best computing time and laser attenuation settings. The registered correlation functions and computed particles mobility's were changed to size distributions and zeta potentials, in that order, utilizing the Malvern Dispersion Software.
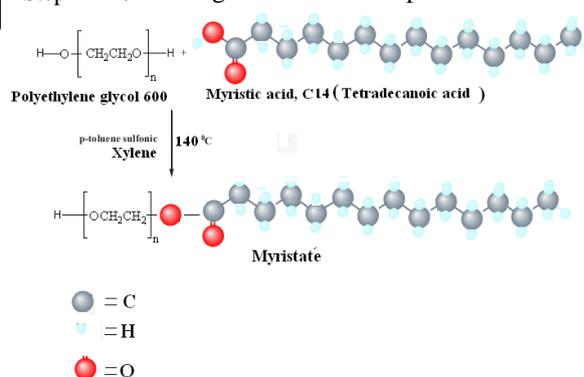
Scheme 2

2.7. Evaluation method of surface active properties:

The tension-active characteristics of the four designed structures were estimated by survey their attitude in aqueous solutions.

2.7.1. Surface tension:

The surface tension of the designed nonionic polymeric surfactants and their nanostructures (Ia, IIa, Ib, and IIb) was set utilizing Du-Nouy Tensiometer (Kruss type 6) at several concentrations scoping from 4×10^{-2} to 1.9×10^{-5} M/L at diverse temperatures 35, 45, 55, 65°C drove by a thermostatic water bath.

_____

_____

2.7.2. Surface criteria of the designed nonionic surfactants:

a) Critical micelle concentration (CMC):

Assign of the critical micelle concentration of the designed surfactants were settled utilizing surface tension strategy. Outcomes of the surface tension estimations were plotted in opposition to the matching concentrations. The break with vary in the SC charts representing the CMC fixations.

b) Effectiveness (π_{CMC}):

π_{CMC} is the variance involving the surface tension of the pure water (γ_o) and the surface tension of the surfactant solution (γ) at the critical micelle concentration.

$$\pi_{CMC} = \gamma_{o} - \gamma_{CMC}$$

c) Efficiency (Pc_{20}):

Efficiency (Pc_{20}) is defined by the concentration (mol/liter) of the surfactant solutions able toward put down the surface tension by 20 dyne/cm.

d) Maximum surface excess Γ_{max}:

The outcomes of the maximum surface excess Γ_{max} estimated from surface or interfacial information through applying of Gibbs equation [24].

$$\Gamma_{max} = - 1 / 2.303 \, RT \; (\delta \gamma / \delta \log C)_{T}$$

Where

Γ_{max} maximum surface excess in mole/cm^2

R   universal gas constant 8.31 x 10^7 ergs mole^{-1} K^{-1}

T   absolute temperature (273.2 + °C)

$\delta \gamma$ surface pressure in dyne/cm

C   surfactant concentration

$(\delta\gamma / \delta \log C)_T$ is the slope of a plot surface tension vs. –log concentration charts under CMC in fixed temperature.

e) Minimum surface area (A_{min}):

The zone for every particle at the interface permits input about the level of pressing and the course of the adsorbed surfactant particle. The mean zone (in square angstrom) required for every one particle adsorbed on the interface [25] is known through:

$$A_{min} = 10^{16} / \Gamma_{max} N$$

A_{min} Minimum surface area in °A^2

Γ_{max} Maximum surface excess in mole / cm^2

N   Avogadro's number 6.023 x 10^{23}

f) Thermodynamic criteria of micellization and adsorption:

The thermodynamic criteria of adsorption and micellization of the designed nonionic surfactants and their nanostructures were estimated through Gibb's adsorption equations as follows:

$$\Delta G^{O}_{mic} = RT \ln (CMC)$$
$$\Delta G^{O}_{ads} = \Delta G^{O}_{mic} - 6.023 \, X10^{-1} \; X \; \pi_{CMC} \; X \; A_{min}$$

$$\Delta S_{mic} = - d (\Delta G^{O}_{mic} / \Delta T)$$
$$\Delta S_{ads} = - d (\Delta G^{O}_{ads} / \Delta T)$$
$$\Delta H_{mic} = \Delta G^{O}_{mic} + T \, \Delta S_{mic}$$
$$\Delta H_{ads} = \Delta G^{O}_{ads} + T \, \Delta S_{ads}$$

2.8. Antimicrobial activity:

The bacteria, _Escherichia coli_ ATCC 23282; _Pseudomonas aeruginosa_ ATCC 10145; _Bacillus subtilis_ ATCC 6633 and _Staphylococcus aureus_ ATCC 35556 were pre- cultured in Luria Bertani (LB) broth. The medium was incubated during the night at 37 °C in rotating shaker incubator.. The media was centrifuged at 10,000 rpm in 5 minutes. The sample was submerged in purified water, and the turbidity was matched to 0.5 McFarland levels to guarantee that the formulation was up to 10^8 cfu/mL. The yeast _Candida albicans_ IMRU 3669 was pre-cultured in yeast malt agar medium for 3 days[26]. Then, the yeast malt agar plates were inoculated with 500 µl of the yeast suspension and left for incubation for 3 days at30 °C (± 1). The alga strain _Chlorella vulgaris_ was grown on BG11 medium according to Rippka et al., (1979),where 100 mL of BG11 broth medium in a 250 mL Erlenmeyer flask was inoculated with the algal cells (OD$_{750}$ 0.1-0.2) and incubated at 26°C (± 1) with shaking at 150 rpm under continuous illumination (2000 LUX) for 3 days. Then, the BG11 agar plates were inoculated with 500 µl of the algal suspension and left for incubation for 3 days at 26°C (± 1).

2.8.1. Germicidal assay:

The germicidal action of the designed polymeric surfactants was tested utilizing dosage equivalent to 5 mg/ml utilizing agar well-diffusion method [27]. Prior to that, by using sterile cotton swab, all of bacteria, yeasts and algal suspension were spread evenly onto the LB, yeast malt and BG11 agar plates, respectively. Then, using a 10-mm cork borer, 4 wells were made on the agar plates and 100 µl of the synthesized polymeric surfactants were added into the wells. The positive control for the bacteria was Erythromycin and for yeast and algae was tetracycline. The negative control for all microorganisms was Dimethyl formamid (DMF). The plates incubated at 37 °C for 24 hours (bacteria) and 28 °C for 72 hours for yeast and algae, respectively. The diameter of inhibition zone was assigned in mm. when utilizing the designed polymeric surfactants.

3. Results and Discussion:

3.1. Structural Characterizations:
FTIR:

FTIR peaks of each the prepared non ionic laurate polyethylene glycol (Ia) & their nanocomposites (Ib)

_____

and myristate polyethylene glycol (IIa), & their nanocomposites (IIb) are similar with a small shift which verify the molecules of the surfactant were accumulated onto the nanoparticles. Figure1a,b was clear that a number of absorption bands such as, the broad bands around 3397 cm^{-1}, is related to the O-H stretching of un-esterified carboxylic acid groups (-COOH) like mentioned by Kooter et al. [20, 28], whereas the bands at 2920-2730 cm^{-1} is due to stretching asymmetric and symmetric vibrations of C-H in that order in aliphatic like mentioned by Hong et al. [20, 29]. The presence of peaks at 2069- 1938 cm^{-1} is related to overtone, whereas the absorption bands at 1627-1536 cm^{-1} are due to C=C, the bending bands of CH$_2$ around 1457-1456 cm^{-1} and a number of medium bands in the region 1400–1200 cm^{-1} was given to the C-H bending and wagging modes, and O–H bending mode. The peaks with strong intensity at 1088-1038 cm^{-1} were related to the C–O bond stretching mode. The band at 2739 cm^{-1} was endorsed to the C–H aliphatic chain stretching mode of the fatty acids. The extreme IR bands at 1728 cm^{-1} and 1248 cm^{-1} assigned to stretching mode of C=O and C-O in that order, of non ionic laurate polyethylene glycol (Ia) & their nanocomposites (Ib) and myristate polyethylene glycol (IIa), & their nanocomposites (IIb) [20].

As shown in the Figure1a,b the FTIR spectra of C12 & C14 with ZnO-NPs (Ib and IIb), the bands were clearly moved to smaller wave numbers with larger value; where, the broad bands around 3397 cm^{-1}& 3499 cm^{-1} respectively, is related to the O-H stretching of un-esterified carboxylic acid groups (-COOH) were obviously travelled to smaller wave numbers of 3390 cm^{-1} & 3407 cm^{-1} respectively, this suggests that such groups have a close interaction with ZnO nanoparticles.

XRD:

X-ray diffraction models of ZnO- EAFD and ZnO-EAFD nanoparticles displayed in Figure2a. The outcomes illustrate that the ZnO-EAFD nanoparticles model shows superior crystallinity, superior intensity and lesser peak width compared with that of the ZnO-EAFD model.

XRD peaks of ZnO-EAFD and ZnO-EAFD nanoparticles appeared at 2θ ~31.67◦, 34.31◦, 36.14◦, 47.40◦, 56.52◦, 62.73◦, 66.28◦, 67.91◦, 69.03◦, 72.48◦ and 76.96◦ were assigned to (100), (002), (101), (102), (110), (103), (200), (112), (201), (004) and (202) of ZnO (Reference Code: 03-065-3411). The peaks of ZnO-EAFD nanoparticles denoted the nanocrystalline existence and corresponded to the clean ZnO regular peaks[30].

XRD examination approved the less/clean of the synthesized ZnO like there would not be another characteristic unclean peaks.Scherrer's formula utilized to compute crystalline dimension of prepared ZnO-EAFD nanoparticles.

$$D = K\lambda/\beta \cos \theta$$

Typically the particle size symbolize as D, Scherer's (0.94) constant symbolize as K, Bragg's equation (2dsinθ = nλ), Wavelength symbolize as be λ, FWHM symbolize as β, and the diffraction angle is symbolized as θ. The crystallite dimensions determined of ZnO-EAFD nanoparticles from Scherrer's formula was in the range of 20 nm, which will be compared with dynamic light scattering particle size measurement.

Figure2b,c of XRD patterns demonstrating the (Ib& IIb) respectively, amorphous nature is greater than ever and resulting in decreasing the crystallinity of ZnO-NPs, wherever the peaks of amorphous diffraction around 2θ =21.31°&2θ =22.30° respectively, are representing the intercalated ZnO-NPs into the surfactant molecules and demonstrates the successful blending.

Figure (1a): FTIR of Esterified PEG with Lauric acid (Ia), and its nanocomposit (Ib)
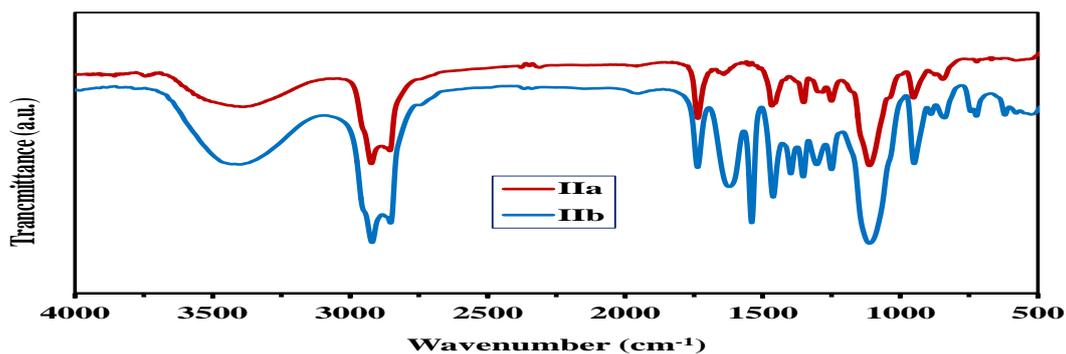
Figure (1b): FTIR of Esterified PEG with Myristic acid (IIa), and its nanocomposite (IIb)
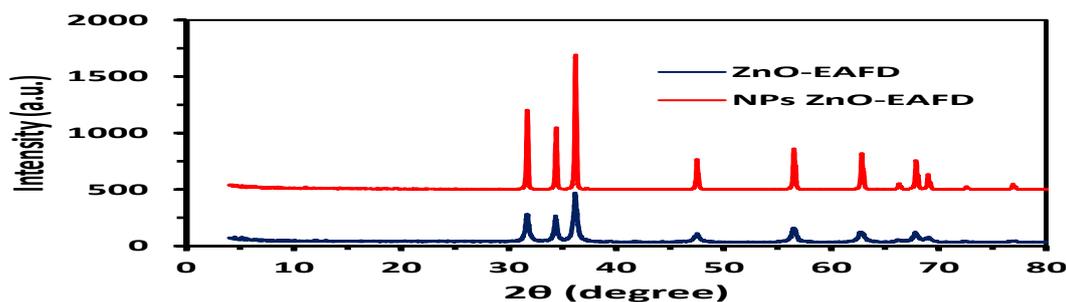
**Fig. (2a): XRD of ZnO-EAFD and NPs ZnO-EAFD**
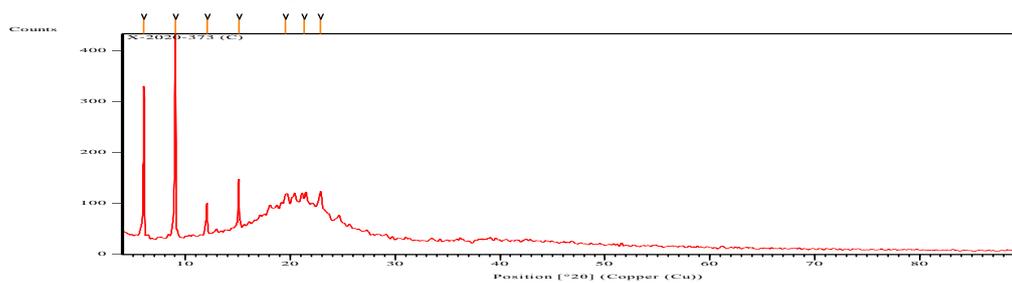

Fig. (2b): XRD of nanocomposite (Ib)
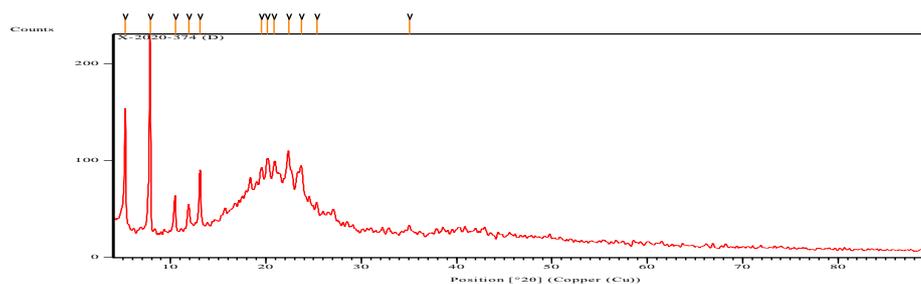
Fig. (2c): XRD of nanocomposite (IIb)

EDAX:

EDAX was used to investigate the chemical profile of ZnO-EAFD NPs. The EDX spectrum of ZnO-EAFD NPs is displayed in Figure 3, which shows four distinct peaks that can be categorized as zinc and oxygen. On the other hands, there are two smaller peaks for nickel and calcium, which may be due to the presence of impurities. As a result, it can be concluded that pure ZnO nanoparticles can be synthesized from EAFD.

BET:

The N_2 adsorption-desorption isotherms and Barret-Joyner-Halenda (BJH) pore size distribution plot of the ZnO- EAFD nanoparticles are shown in Figure 4. The isotherm is capable of classified as a category IV isotherm with a category H4 hysteresis

loop in the P/P0 range of 0.4-0.9, according to the IUPAC classification. The BJH distribution plot displayed in inset of Figure 6 appears the presence of an initial pore size distribution peak focused at ~3.66 nm and a minor distribution peak focused at 6.67 nm.

All such outcomes point toward the mesoporous kind of the engineered ZnO- EAFD nanoparticles. The BET surface area of the ZnO-EAFD nanoparticles is measured to be 58.9 m^2 /g.
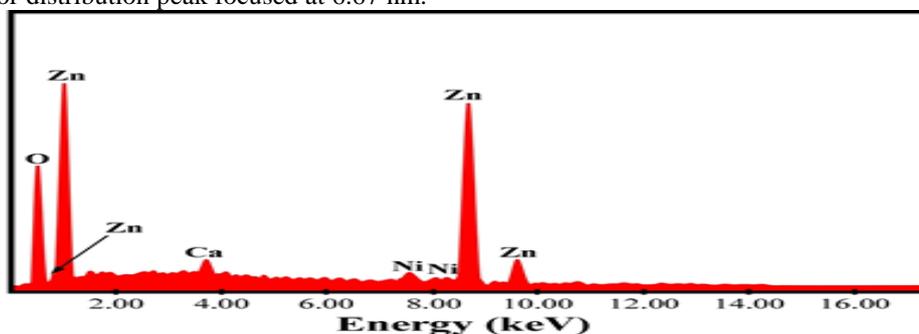

Fig. (3): EDAX of NPs ZnO-EAFD
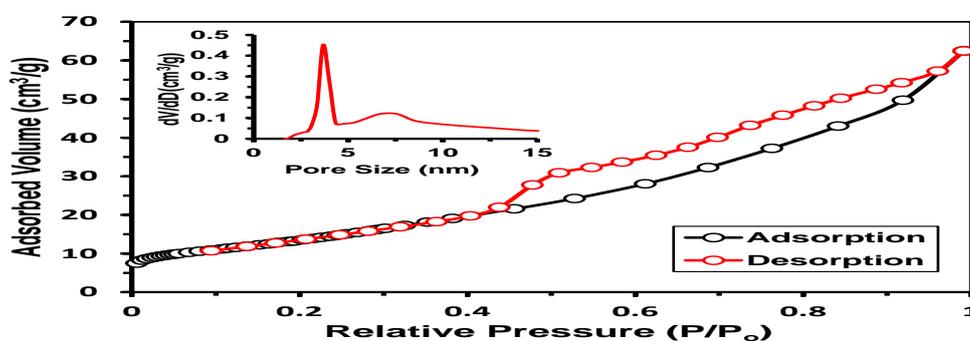
Fig. (4): BET and pore size of NPs.ZnO-EAFD

DLS Analysis:

It showed that the diameter calculated in DLS method points to how a particle can distribute inside a medium; thus, it points to a hydrodynamic diameter. Depending on the outcomes of dynamic light scattering studies, it is discovered that each polymeric surfactant solution and its composites have only one peak like displayed in Figure 5b-e. Obviously the polymeric surfactants in aqueous solutions possess in common a powerful ability to accumulate and shape large agglomerates when increase the number of surfactant carbon, Fig.5$_{b,c}$ respectively, and as blending them with ZnO NPs, Fig.5$_{d,e}$ respectively. It may be interpreted by a greater level of complexity of particles as a result of particles conformational modification in solution.

3.2. Tensiometric parameters:

The designed nonionic polymeric surfactants and their nanostructures Ia, IIa, Ib and IIb were assessed as surface active agents by estimate the surface tension of their aqueous solutions at variety of temperatures 35, 45, 55 and 65 ºC utilizing a surface tension system and the outcomes are depicted in Figure 6. It is well known that a considerable drop of the surface tension occurred with growing the concentration of the designed surfactants which

explained on the basis of movement of the surfactant particles from the bulk of the solution pointed to the interface [31].

Particularly, the hydrophobicity of the investigated designed structures has a significant impact on the surface tension fall of the surfactants at the equivalent concentration. Therefore, the structure IIa that comprise a taller hydrophobic chain and its nanostructure IIb demonstrate a worse reduction in the surface tension comparing with structure Ia and its nanostructure Ib, as a result of a great trend of the more hydrophobic structure to adsorption at the air/water interface, due to maximize the hydrophobicity exhibit more disagreement among the polar system and the hydrophobic chains because the variation in their polarity. The self-assembly of the designed surfactants on the surface of the zinc oxide nanoparticles stabilizes their nano size which avoids their aggregation as a result of the generation of nano shells with the surfactants and the aggregation reduced significantly as the alkyl chain length growing due to rise the space among the generated nanostructures. In addition, there is a drop in the surface tension as the temperatures growing from 30 to 60 ºC, as a result of dehydration of hydrophilic parts that cause diminish of the solubility of surfactants to collect in the surface.
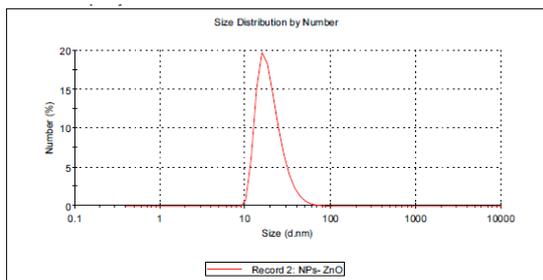
Fig. (5a): DLS of ZnO-NPs
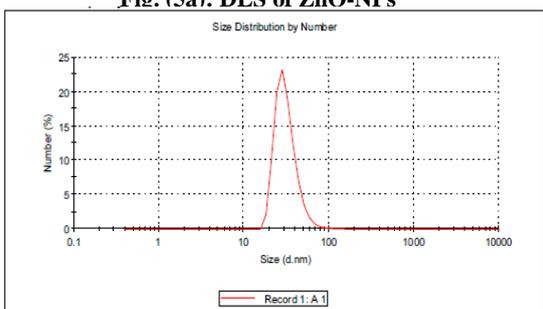
Fig. (5b): DLS of esterified PEG (Ia)
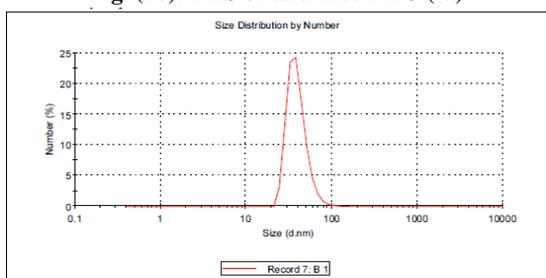
Fig. (5c): DLS of esterified PEG (IIa)
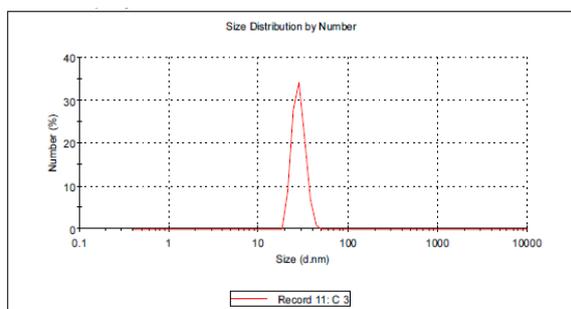
Fig. (5d): DLS of nanocomposite (Ib)
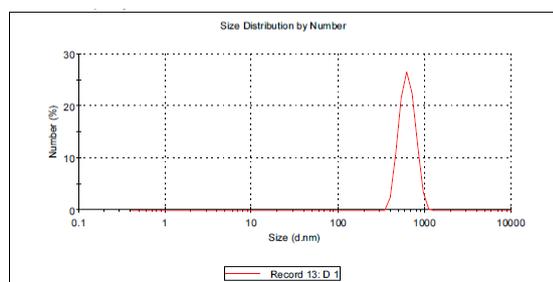
Fig. (5e): DLS of nanocomposite (IIb)
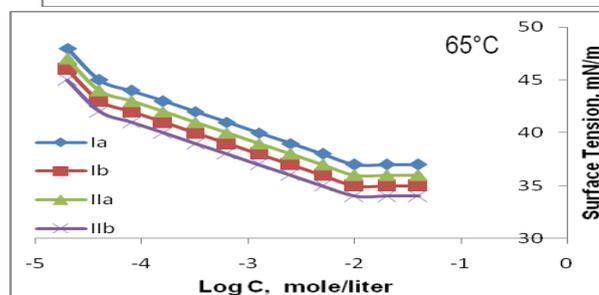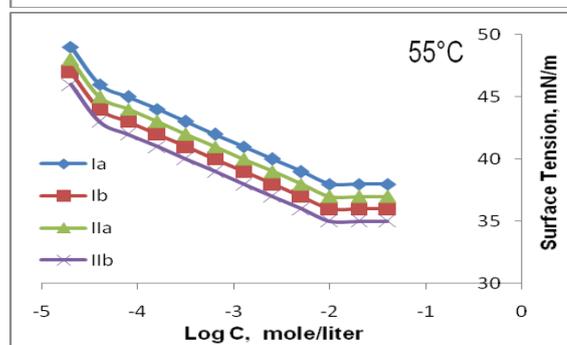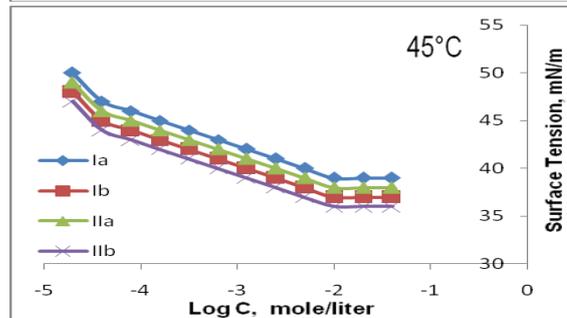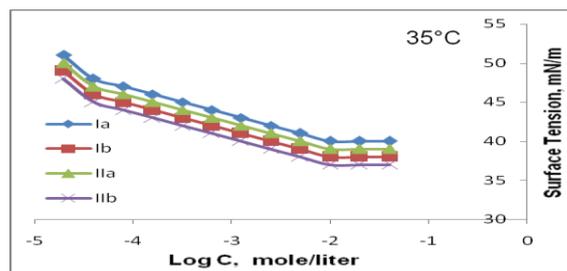
Fig. (6): Surface tension vs. log concentration of synthesized polymeric surfactants and their nano-structures at: (a) 35 ºC, (b) 45 ºC, (c) 55 ºC, (d) 65 ºC.

The surface tension outcomes of the nanostructures of the designed surfactants with ZnO nanoparticles exhibited lower values comparing with the individual surfactants that indicates the grow in the solubility of the designed structure after assembling on metal nanoparticles and the greatest lessening of surface tension achieved by the nanostructure of the synthesized myristate surfactant (IIb) than other designed structures.

The scores of the CMC for the designed surfactants were assigned at several temperatures 35, 45, 55 and

65°C. Interception of the pre-and post-micellar patterns at the breakpoints of two straight lines matched to the concentration range marked by a linear decrease in surface tension (γ) and to the near-constant surface tension concentration region; Table 1.The estimation of CMC is known to be a critical factor since nearly all of the physical and chemical characteristics of the surfactant solutions express sudden variety at this concentration. It is clear that the CMC results illustrate a reduction in the CMC by a raise in the extent of the hydrophobic chains; however, growing the hydrophobic component reduces the solubility contributing to the buildup of the surfactant particles on the surface and to the development of micelles.

In the other side, when the temperature increment, the CMC minimizes, this is because the reduction in the hydration of the hydrophilic moieties, that strengthens the micellization. In the opposite, there is a disarrangement of the normal water molecules bordering the hydrophobic moieties as the temperature rises and the micillization is unloved. As seen in table (3), the CMC results diminished as temperatures maximized, i.e. enhance in micellization occurred. CMC results also indicate the potential of the formulated surfactant and its nanocomposites to dissolve in water. The minimum CMC scores were observed for nanocomposites that show an improvement in the solubility of the designed surfactant after assembly on ZnO nanoparticles [32].

The surface tension of the surfactant solution at the CMC assign the effectiveness thus, growing the hydrophobicity of the designed surfactants raises the reduction of the surface tension at the interface, whereas the efficiency (P_{C20}) i.e the concentration of surfactant necessary to obtain a 20 mN m^{-1} depression in surface tension, is minimized. At such a level, the concentration of the surfactant is near to the minimum concentration required to achieve the optimum adsorption at the interface. The maximum surface excess, Γ_{max}, is considered a significant feature to screen the surface action of the designed surfactant particles at the interface that might be assessed by utilizing the Gibbs adsorption isotherm, by growing the hydrophobicity; the scores of maximum surface excess at the interface are raised representing advanced surface concentration due to rise the trend of adsorption of surfactant particles because growing the hydrophobic character of the particles.

The minimum surface area scores engaged with the designed nonionic surfactants and their nano-structures at the interface, A_{min}, (nm^2), when the surface adsorption was fully busy, by considering the minimum surface area (A_{min}) a main data concerning the orientation mode of the surfactant particles at the interface may be achieved. Growing the number of adsorbed particles at the interface cause develop the scores of the maximum surface excess, therefore the zone accessible for each particle might diminish. Consequence a thick compacting film of surfactant particles are created at the interface.

The scores of CMC, π_{CMC}, P_{C20}, Γ_{max} and A_{min} existed in table 1. In a few words, it is obviously revealed that compound IIb accomplished the specified results of the surface tension at a minor concentration as matched with other designed structures. Accordingly, it can be understood that compound IIb is extra tensio-active than compounds Ia, Ib and IIa and informative much better surface properties.

3.3. Thermodynamic of micellization and adsorption:

The standard free energies of adsorption and micellization (ΔG°_{ads} and ΔG°_{mic}) at 35, 45, 55 and 65 °C were utilized to investigate the thermodynamic manner of the designed surfactants in their solutions.

The records of the thermodynamic characteristics of micellization and adsorption were put in Tables 2, 3. Evidently, it can be noticed from the tables that the records of the standard free energies of adsorption and micellization of the designed surfactants have constantly negative scores. The condition points to the adsorption and micellization operations together run naturally. Furthermore, the standard free energies of adsorption of designed structures at the air/water interface gave extra negative scores compared with the scores of the micellization showed to the adsorption course is further approving than the micellization. Additionally, the great variation among ΔG°_{ads} and ΔG°_{mic} records can be interpreted based on the adsorbed particles at the interface are tightly packed; accordingly, the water particles isn't react considerably through all such particles [33].

3.4. Biological action of the designed compounds:

The results of the study in Table (4) and Figure (7) showed that polymeric nonionic surfactants and their nanostructures possess antimicrobial activity by showing the inhibition zone around the wells. However, among all microorganisms tested only *Staph. aureus* showed high inhibition zone (40 mm) at the studied nanostructures (Ib) and (IIb) compared to the positive control (28 mm), respectively. Meanwhile, *Bacillus subtilis* showed higher inhibition zone (45 mm) at the nonionic surfactant nanostructure (IIb). There were no zones of inhibition recorded against *Candida albicans*. Moreover, in this study the nanostructure of the polymeric nonionic surfactants (Ib) and (IIb) showed more effective against Gram-positive bacteria (*Bacillus subtilis* and *Staph. aureus*) compared to Gram-negative bacteria (*P. aeruginosa* and *E.coli*), yeast (*Candida albicans*) and microalga (*Chlorella Vulgaris*).

_____

Table (1): Surface properties of synthesized compounds at 35, 45, 55, 65 °C.

Surfactant		CMC X 10^{-3}, Mole/liter	π_{CMC}, mN/m	Γ_{max} X 10^{-11}, Mole/cm^2	A_{min}, nm^2
Ia		5	31	6.4	2.59
Ib		3.9	32.5	6.59	2.53
IIa	**35 °C**	4.5	31.5	6.58	2.52
IIb		3.2	33.5	6.6	2.5
Ia		4.3	31.5	6.37	2.61
Ib		3.4	33.5	6.38	2.6
IIa	**45 °C**	3.6	32.5	6.38	2.6
IIb		2.7	35	6.4	2
Ia		3.4	32.5	6.18	2.7
Ib		2.7	34	6.19	2.6
IIa	**55 °C**	3.1	33.5	6.19	2.68
IIb		2.2	34.5	6.45	2.57
Ia		3	33.5	6	2.8
Ib		2.5	35	6.1	2.76
IIa	**65 °C**	2.8	34	6.1	2.76
IIb		2.1	35.5	6.26	2.65

Table (2): Thermodynamic parameters of micellization of synthesized compounds at 35, 45, 55, 65 °C.

Surfactant		ΔG^O_{mic}, KJ/mole	ΔH_{mic}, KJ/mole
Ia		-39.14	-39.14
Ib		-39.16	-39.16
IIa	**35 °C**	-45.88	-45.88
IIb		-43.1	-43.1
Ia		-40.81	-40.81
Ib		-40.79	-40.79
IIa	**45 °C**	-47.96	-47.96
IIb		-44.9	-44.9
Ia		-43	-43
Ib		-39.42	-39.42
IIa	**55 °C**	-40.68	-40.68
IIb		-37.68	-37.68
Ia		-44.04	-44.04
Ib		-40.83	-40.83
IIa	**65 °C**	-42.21	-42.21
IIb		-38.96	-38.96

Table (3): Thermodynamic parameters of adsorption of synthesized compounds at 35, 45, 55, 65 °C.

Surfactant		ΔG^O_{ads}, KJ/mole	ΔH_{ads}, KJ/mole
Ia		-61.91	-123.6
Ib		-63.72	-179.3
IIa	**35 °C**	-61.64	-188.6
IIb		-65.14	-146.5
Ia		-63.91	-127.6
Ib		-67.47	-186.8
IIa	**45 °C**	-65.76	-196.9
IIb		-67.78	-141.8
Ia		-68.34	-215
Ib		-69.36	-254.5
IIa	**55 °C**	-69.81	-174.5
IIb		-70.08	-197.7
Ia		-72.81	-224
Ib		-75	-265.7
IIa	**65 °C**	-73	-181
IIb		-73.97	-205.5

_____
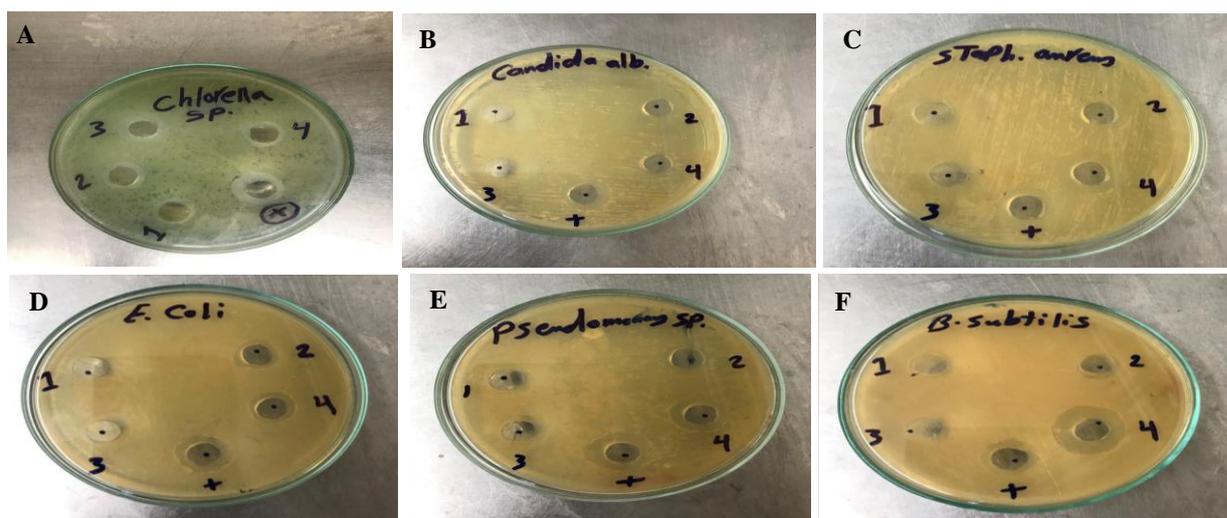
Figure (7): **Antimicrobial activity of tested polymeric nonionic surfactants and their nanostructures [1 = (Ia); 2 = (IIa); 3 = (Ib); 4 = (IIb); + = positive control] on different microbes [(A) =** *Chlorella Vulgaris,* **(B)=** *Candida albicans,* **(C)=** *Staph. aureus* **, (D) =** *E. coli,* **(E)=** *P. aeruginosa* **and (F)=** *Bacillus subtilis***].**

These results parallel to other previous study [34,35] that claimed the nanostructure of the nonionic surfactants were highly successful towards Gram-positive bacteria but shorter against Gram-negative bacteria. Basically, the variation between the two antimicrobial actions perhaps due to the dissimilarity in the cell walls of the bacteria. The cell film of Gram-positive bacteria just contains an external peptidoglycan sheet. Because of this structure, it is extra penetrable to further materials.

While, the external layer of the cell film of the Gram negative bacteria comprised of lipopolysaccharides. These structures make it minimally penetrable to further materials [36]. Bacterial cell wall of Gram-positive bacteria is composed of 90-95% peptidoglycan and only 5-10% of lipid [37]. Less percentage of lipids caused less rigidity in bacterial cell wall. However, in Gram-negative bacteria, 90-95% of its bacterial cell wall composed of lipid and 5-10% of peptidoglycan.

Thus, this might explain the reason why Gram-negative bacteria have a resistance towards nonionic surfactants in comparison with Gram-positive bacteria. Any particle that enters a living organism is continuously joined to its cell wall. This connection may cause an alteration in the substrate itself, which could toxically influence the film that may cause damage or even decimation, responsible for the death of the organism. As a consequence of being polar groups in the skeleton of nonionic surfactants, they appear to accumulate in the cell wall and reduce their osmotic length motivating the microorganism to die. The germicidal action of the biocide counts on its molecular structure [38, 39]. As appeared in table (4) the designed polymeric nonionic surfactants and their

nanostructures Ia, IIa, Ib and IIb have high-quality biological action touching the investigated microorganisms. As a consequence of their protocol, nonionic surfactants are known to be one of the potent biocides. Oxygen atoms, owing to their electronegativity, had to near the connecting field. In addition to the hydrophobic moieties, along with the electrostatic forces, the substantial proteins that encircle the substrate of the cell must be encapsulated in the hydrogen bonding situation. In particular, hydrogen bonding is programmed to destabilize the cell membrane. The hydrophilic portion of the cell wall bound to the hydrophilic portion of the nonionic surfactant (polyethoxy) by means of an intermolecular hydrogen bond. This seems to be the antimicrobial powerful form as a surfactant, the bounded location of the biocide is unclear [40]. Rising the concentration of the biocide heading to extra gathering in the different substrates (aqueous or microorganism membranes) [41]. Therefore, a greater set of nonionic surfactants in the layer of cells improves the amount strong motion of particles in the path of microorganisms. The suppression capacity of nanocomposites is greater than that of single surfactants. While the improvement in biological action of the designed surfactant with nanoparticles can be attributed to the existence of little-sized nanoparticles and a high surface-to-volume ratio in the nanostructures of the designed surfactants, which enables them to touch directly with microbial wall, which enhance the diffusion of the surfactant particles into the cell membrane of the microorganism.

6932

A. I. Adawy et.al.
_____

Table (4): The results of biological activity of the synthesized polymeric surfactant and their nano-structures 5mg/ml against different microorganisms measured by mm.

organisms Samples	*Bacillus subtilis*	*Staph. aureus*	*Escherichia coli*	*Pseud. aeruginosa*	*Candida albicans*	*Chlorella sp.*
(Ia)	**10**	**10**	**10**	**10**	**Nil**	**8**
(IIa)	10	10	10	10	Nil	11
(Ib)	50	40	15	10	Nil	16
(IIb)	45	40	10	15	Nil	10
control	29	28	28	30	27	28

4. Conclusion:

Based on polyethylene glycol, the nonionic polymeric surfactants Ia and IIa and their nanostructures Ib and IIb were prepared and pointed up. In addition, ZnO nanoparticles derived as of hazardous trash "Electric Arc Furnace Dust (EAFD)" was prepared and characterized. Also, it was investigated the surface attitude of the designed surfactants and their nanostructures in aqueous medium using surface tension detecting that they have good surface activity and the nanostructure of the synthesized myristate surfactant (IIb), with longer hydrophobic chain length had the lowest critical micelle concentration also the micellization affinity increases with maximize the temperature. In conclusion, the synthesized nonionic polymeric surfactants gave good biological activity against different microorganisms and blending these prepared polymeric surfactants with ZnO nanoparticles to obtain polymeric surfactants nanocomposites for enhancing their biological activity, where the surface parameters play an important role in their antimicrobial effect.

Conflict of Interest

The authors declare that they have no known competing financial interests or personal relationships that could have appeared to influence the work reported in this paper.

References

[1] Shaban S.M., Elsamad S.A., Tawfik S.M., Abdel-Rahman A.A.-H. and Aiad I., Studying surface and thermodynamic behavior of a new multi-hydroxyl Gemini cationic surfactant and investigating their performance as corrosion inhibitor and biocide. *Journal of Molecular Liquids,* **316**, 113881 (2020). https://doi.org/10.1016/j.molliq.2020.113881

[2] Smułek W., Burlaga N., Hricovíni M., Medveďová A., Kaczorek E. and Hricovíniová Z., Evaluation of surface active and antimicrobial properties of alkyl D-lyxosides and alkyl L-rhamnosides as green surfactants. *Chemosphere*, **271**, 129818 (2021). https://doi.org/10.1016/j.chemosphere.2021.129818

[3] Labena A., Hamed A., Ismael E.H.I. and Shaban S.M. Novel Gemini Cationic Surfactants: Thermodynamic, Antimicrobial Susceptibility, and Corrosion Inhibition Behavior against Acidithiobacillus ferrooxidans. *J Surfactants Deterg*, **23**, 991-1004 (2020). https://doi.org/10.1002/jsde.12437

[4] Hegazy M.A. and El-Agamy H.H., ICMMS-2: Synthesis and Characterization of ZnO Nanoparticles in Presence of Triethanolamine (TEA) as Surfactant Via Sol-Gel. *Egypt. J. Chem*, (2021). https://doi.org/10.21608/ejchem.2021.55874.3189

[5] Adawy A.I., Abdeen Z.I., Abdel Rahman N.R. and Ali H.E.-S., Evaluation of the biological activity of the prepared nonionic polymeric based on the acrylated polyethylene glycol. *Journal of Molecular Liquids,* **288**, 111010 (2019). https://doi.org/10.1016/j.molliq.2019.111010

[6] Tawfik S.M., Negm N.A., Bekheit M., Abd El-Rahman N.R. and Abd-Elaal A.A., Synergistic interaction in cationic antipyrine/CTAB mixed systems at different phases. *Journal of Dispersion Science and Technology,* 1–11 (2021). https://doi.org/10.1080/01932691.2021.1878899

[7] Betiha M.A., El-Henawy S.B., Al-Sabagh A.M., Negm N.A. and Mahmoud T., Experimental evaluation of cationic-Schiff base surfactants based on 5-chloromethyl salicylaldehyde for improving crude oil recovery and bactericide. *Journal of Molecular Liquids,* **316**, 113862 (2020). https://doi.org/10.1016/j.molliq.2020.113862

[8] Abdeen Z.I. and Ghoneim A.I., Improving of the Mg-Co nanoferrites efficiency for crude oil adsorption from aqueous solution by blending them with chitosan hydrogel. *Environ Sci Pollut Res.,* **27**, 19038–19048 (2020). https://doi.org/10.1007/s11356-018-3557-y

[9] Badr E.A., Shafek S.H., Hefni H.H.H., Elsharif A.M., Alanezi A.A., Shaban S.M. and Kim, D.-H., Synthesis of Schiff base-based cationic Gemini surfactants and evaluation of their effect on in-situ AgNPs preparation: Structure, catalytic, and biological activity study. *Journal of Molecular*

Liquids, **326**, 115342 (2021). https://doi.org/10.1016/j.molliq.2021.115342

[10] Morsi R.E. and El-Salamony R.A., Effect of cationic, anionic and non-ionic polymeric surfactants on the stability, photo-catalytic and antimicrobial activities of yttrium oxide nanofluids. _Journal of Molecular Liquids,_ **297**, 111848 (2020). https://doi.org/10.1016/j.molliq.2019.111848

[11] Kalaycioglu G.D. and Aydogan N., Fluorocarbon/ hydrocarbon hybrid surfactant decorated gold nanoparticles and their interaction with model cell membranes. _Journal of Molecular Liquids,_ **326**, 115346 (2021). https://doi.org/10.1016/j.molliq.2021.115346

[12] Elged A.H., Shaban S.M., Eluskkary M.M., Aiad I., Soliman E.A., Elsharif A.M. and Kim D.-H., Impact of hydrophobic tails of new phospho-zwitterionic surfactants on the structure, catalytic, and biological activities of AgNPs. _Journal of Industrial and Engineering Chemistry,_ **94**, 435–447 (2021). https://doi.org/10.1016/j.jiec.2020.11.017

[13] El-Shamy O.A.A., Habib A.O., Mohamed D.E. and Badawi A.M., Synthesis, Characterization, Surface, and Thermodynamic Studies of Alkyl Tetrachloro ferrates: Performance Evaluation of Their Nanostructures as Biocides. _J Surfactants Deterg,_ **23**, 215–223 (2020). https://doi.org/10.1002/jsde.12349

[14] Wang Y., Zhang Q., Zhang C. and Li P., Characterisation and cooperative antimicrobial properties of chitosan/nano-ZnO composite nanofibrous membranes. _Food Chemistry.,_**132**, 419–427 (2012). https://doi.org/10.1016/j.foodchem.2011.11.015

[15] El-Nemr K.F., Mohamed H.R., Ali M.A., Fathy R.M. and Dhmees A.S., Polyvinyl alcohol/gelatin irradiated blends filled by lignin as green filler for antimicrobial packaging materials. _International Journal of Environmental Analytical Chemistry,_ **100**, 1578–1602 (2020). https://doi.org/10.1080/03067319.2019.1657108

[16] Ibrahim M.M., El-Sheshtawy H.S., Abd El-Magied M.O.and Dhmees A.S., Mesoporous Al $_2O_3$ derived from blast furnace slag as a cost-effective adsorbent for U(VI) removal from aqueous solutions. _International Journal of Environmental Analytical Chemistry,_ 1–17 (2021). https://doi.org/10.1080/03067319.2021.1900150

[17] Amdeha E., Mohamed R.S. and Dhmees A.S., Sonochemical assisted preparation of ZnS–ZnO/MCM-41 based on blast furnace slag and electric arc furnace dust for Cr (VI) photoreduction. _Ceramics International,_ S0272884221013821 (2021). https://doi.org/10.1016/j.ceramint.2021.05.015

[18] Dhmees A., Rashad A. and Abdullah E., Calcined Petroleum Scale- CaO a Cost-Effective Catalyst for Used Cooking Oil Methanolysis. _Egypt. J. Chem,_ **63**, 1033-1044 (2020). https://doi.org/10.21608/ejchem.2019.15107.1912

[19] Deyab M.A., Corrêa R.G.C., Mazzetto S.E., Dhmees A.S. and Mele G., Improving the sustainability of biodiesel by controlling the corrosive effects of soybean biodiesel on aluminum alloy 5052 H32 via cardanol. _Industrial Crops and Products,_ **130**, 146–150 (2019). https://doi.org/10.1016/j.indcrop.2018.12.053

[20] Adawy A.I., Ghoneim A. and Abdeen Z., Enhancement of the Biological Activity for Esterified Polyethylene Glycols by Blending them with Sr –Co Nanoferrites, (under publication).

[21] Youcai Z.and Stanforth R., Integrated hydrometallurgical process for production of zinc from electric arc furnace dust in alkaline medium. _Journal of Hazardous Materials,_ **80**, 223–240 (2000). https://doi.org/10.1016/S0304-3894(00)00305-8

[22] Morcali M.H., Reductive atmospheric acid leaching of spent alkaline batteries in H2SO4/Na2SO3 solutions. _Int J Miner Metall Mater,_ **22**, 674–681 (2015). https://doi.org/10.1007/s12613-015-1121-z

[23] Negm N.A., Tawfik S.M. and Abd-Elaal A.A., Synthesis, characterization and biological activity of colloidal silver nanoparticles stabilized by gemini anionic surfactants. _Journal of Industrial and Engineering Chemistry,_ **21**, 1051–1057 (2015). https://doi.org/10.1016/j.jiec.2014.05.015

[24] Rosen M.J., Surfactants and Interfacial Phenomena. John Wiley & Sons, Inc., Hoboken, NJ, USA (2004)

[25] El-Sukkary M.M.A., Shaker N.O., Ismail D.A., Ahmed S.M. and Awad A.I., Preparation and evaluation of some amide ether carboxylate surfactants. _Egyptian Journal of Petroleum,_ **21**, 11–17 (2012). https://doi.org/10.1016/j.ejpe.2012.02.002

[26] Zaky A.S., Gregory A. Tucker, Daw Z.Y. and Du C., Marine yeast isolation and industrial application. _FEMS Yeast Res,_ **14**, 813–825 (2014). https://doi.org/10.1111/1567-1364.12158

[27] Shaban S.M., Aiad I. and Ismail A.R., Surface Parameters and Biological Activity of N(3-(Dimethyl Benzyl Ammonio) Propyl) Alkanamide Chloride Cationic Surfactants. _J. Surfactants Deterg.,_**19**, 501–510 (2016), https://aocs.onlinelibrary. wiley.com /doi/full/10.1007/s11743-016-1795-x

[28] Kooter I.M., Pierik A.J., Merkx M., Averill B.A., Moguilevsky N., Bollen A. and Wever R., Difference Fourier Transform Infrared Evidence for Ester Bonds Linking the Heme Group in Myeloperoxidase, Lactoperoxidase, and Eosinophil Peroxidase. _J. Am. Chem. Soc,_ **119**, 11542–11543 (1997). https://doi.org/10.1021/ja9725460

[29] Hong R.-Y., Li J.-H., Zhang S.-Z., Li H.-Z., Zheng Y., Ding J. and Wei D.-G., Preparation and characterization of silica-coated Fe3O4 nanoparticles used as precursor of ferrofluids. _Applied Surface Science,_ **255**, 3485–3492 (2009). https://doi.org/10.1016/j.apsusc.2008.09.071

[30] Dhmees A., Hegazey R. and Alazabawy R., Preparation of cost-effective photodegradation catalyst based on zinc oxide derived from electric arc furnace dust and kaolinite. _Current Research in Psychology,_ **11**, 5840–5846 (2019). https://doi.org/10.24941/ijcr.36089.07.2019

_____

[31] Negm N.A., El Hashash M.A., Youssif M.A., Ismail E.A., Abdeen Z.I. and Rahman N.R.A., Novel Nonionic Polyurethane Surfactants and Ag Nanohybrids: Influence of Nonionic Polymeric Chains. *J Surfact Deterg,* **20**, 173–182 (2017). https://doi.org/10.1007/s11743-016-1909-5

[32] Azzam E.M.S. and Zaki M.F., Surface and antibacterial activity of synthesized nonionic surfactant assembled on metal nanoparticles. *Egyptian Journal of Petroleum,* 25, 153–159 (2016). https://doi.org/10.1016/j.ejpe.2015.04.005

[33] Adawy A.I. and Khowdiary M.M., Structure and Biological Behaviors of Some Metallo Cationic Surfactants. *Journal of Surfactants and Detergents,* **16**, 709–715 (2013).https://doi.org/10.1007/s11743-013-1483-z

[34] Wieczorek D., Gwiazdowska D., Michocka K., Kwaśniewska D. and Kluczyńska K., Antibacterial activity of selected surfactants. *Polish J Commodity Sci.,* **38**, 142–149 (2014)

[35] Hui A., Yan R., Mu B., Kang Y., Zhou Y. and Wang A., Preparation and Antibacterial Activity of ZnO/Palygorskite Nanocomposites Using Different Types of Surfactants. *Journal of Inorganic and Organometallic Polymers and Materials,* **30**, 3808–3817 (2020). https://doi.org/10.1007/s10904-020-01613-7

[36] Afifah S. N., Darah I., Fariza S. S., Nordin M. M. J. and Aili Z. N., Antimicrobial Activity of Various Extracts of a Tropical Chlorophyta Macroalgae, Halimeda discoidea , *Journal of Applied Sciences,* **10**(23), 3007-3013 (2010) https://scialert.net/abstract/?doi=jas.2010.3007.3013

[37] Shafay S.M.E., Ali S.S. and El-Sheekh M.M., Antimicrobial activity of some seaweeds species from Red sea, against multidrug resistant bacteria. *Egyptian Journal of Aquatic Research,* **42**, 65–74 (2015)

[38] Pérez L., Pinazo A., Teresa G.M., Lozano M., Manresa A., Angelet M., Pilar V.M., Mitjans M., Pons R. and Rosa I.M., Cationic surfactants from lysine: Synthesis, micellization and biological evaluation. *European Journal of Medicinal Chemistry,* **44**, 1884–1892 (2009). https://doi.org/10.1016/j.ejmech.2008.11.003

[39] Alsahib S.A. and Dhedan R.M., Synthesis and Characterization of some Tetrazole Derivatives and Evaluation of their Biological Activity. *Egypt. J. Chem.,* **64**, 14-15 (2021). https://doi.org/10.21608/ejchem.2021.54356.3165

[40] Tawfik S.M., Zaky M.F., Mohammad T.G.M. and Attia H.A.E., Synthesis, characterization, and in vitro antifungal activity of anionic and nonionic surfactants against crop pathogenic fungi. *Journal of Industrial and Engineering Chemistry,* **29**, 163–171 (2015). https://doi.org/10.1016/j.jiec.2015.03.031

[41] Aiad I.A., Badawi A.M., El-Sukkary M.M., El-Sawy A.A. and Adawy A.I., Synthesis and Biocidal Activity of Some Naphthalene-Based Cationic Surfactants. *J Surfact Deterg,* **15**, 223–234 (2012). https://doi.org/10.1007/s11743-011-1286-z.

_____